Nuclear Science and Techniques (2023) 34:97
https://doi.org/10.1007/s41365-023-01248-6

RESEARCH HIGHLIGHT

Hypernuclei as a laboratory to test hyperon–nucleon interactions

Yu-Gang Ma[1,2]

Published online: 27 June 2023

Directed flow (v_1) of the hypernuclei ${}^{3}_{\Lambda}\mathrm{H}$ and ${}^{4}_{\Lambda}\mathrm{H}$ have been observed in mid-central Au+Au collisions at $\sqrt{s_{\mathrm{NN}}}$ = 3 GeV at RHIC. This measurement opens up a new possibility for studying hyperon–nucleon (*Y*–*N*) interaction under finite pressure. In addition, multi-strangeness hypernuclei provide a venue to probe hyperon–nucleon–nucleon (*Y*–*N*–*N*) and even hyperon–hyperon–nucleon (*Y*–*Y*–*N*) interactions. Hypernuclei are important for making connection between nuclear collisions and the equation of state which governs the inner structure of compact stars.

Hypernucleus, a bound state of hyperon(s) and nucleons, is a "laboratory" to study the hyperon–nucleon (*Y*–*N*) interactions. The strength of *Y*–*N* interaction is fundamentally important for understanding the nature of strong interaction. Based on simple kinematics, the theory predicts that the hyperon would exist in the interior of neutron star, which is the collapsed core of a massive star (around 10–25 solar mass), and has a typical mass of 1–2 solar mass and a radius of 10–12 km. However, the equation of state (EoS) with including strangeness were essentially excluded by the observations of massive neutron stars (*e.g.* PSR J0740-6620 [1]), due to that the presence of hyperons in the core of neutron star would soften the EoS. This inconsistency of theory and observations is the so-called "hyperon puzzle". To allow the existence of observed two-solar-mass neutron star with including hyperons, theory suggests that *Y*–*N* and *Y*–*N*–*N* interaction at high baryon density can create a stiffer EoS which can compensate the mentioned soften effect. Therefore, nuclear matter density dependent *Y*–*N* and *Y*–*N*-*N* interaction deduced experimentally is highly expected to the communities of nuclear physics and astrophysics.

High energy heavy-ion collision provides an effective tool to create hot dense nuclear matter [2, 3] which finally evolves to form various particles and rare nuclei in the laboratory [4–9], providing a venue to study the strong interaction [10–14]. Thermal model [15] and hadronic transport model with coalescence afterburner [16, 17] calculations have predicted abundant production of light hypernuclei in high-energy nuclear collisions, especially at high baryon density. Collective flow is driven by pressure gradients created in such collisions, which has been commonly used for studying the properties of nuclear matter created in collisions. Due to its genuine sensitivity to early collision dynamics [18–28], the first order coefficient of the Fourier-expansion of the azimuthal distribution in the momentum space, v_1, also called the directed flow, has been analyzed for many particles species ranging from π-mesons to light nuclei for a long time [29–34], see a carton picture in Fig. 1. Hence, measurements of hypernuclei collective flow help to study the *Y*–*N* interactions in the QCD equation of state at high baryon density.

Now publishing in *Physical Review Letters* [35], the STAR Collaboration has reported the first observation of directed flow, v_1, of ${}^{3}_{\Lambda}\mathrm{H}$ and ${}^{4}_{\Lambda}\mathrm{H}$ in center-of-mass energy $\sqrt{s_{\mathrm{NN}}}$ = 3 GeV Au + Au collisions. The work was mainly contributed by a joint team of Institute of Modern Physics (IMP@CAS) and Lawrence Berkeley National Laboratory, led by Xin Dong, Xionghong He, Chenlu Hu, Yuanjing Ji, Yue-Hang Leung, Nu Xu, Yapeng Zhang, and Fengyi Zhao.

The data were collected by the STAR experiment at Relativistic Heavy-Ion Collider (RHIC) with the fixed-target (FXT) setup in 2018. A gold beam of energy at 3.85*A* GeV is bombarded on a gold target of thickness 1% interaction length. After colliding vertex selection, a total of 2.6×10^{8}

The author thanks Yapeng Zhang and Liang Zhang for communications. His work is supported by supported in part by the National Natural Science Foundation of China (Nos. 11890714 and 12147101), and the Guangdong Major Project of Basic and Applied Basic Research (No. 2020B0301030008).

✉ Yu-Gang Ma
mayugang@fudan.edu.cn

[1] Key Laboratory of Nuclear Physics and Ion-beam Application (MOE), Institute of Modern Physics, Fudan University, Shanghai 200433, China

[2] Shanghai Research Center for Theoretical Nuclear Physics, NSFC and Fudan University, Shanghai 200438, China

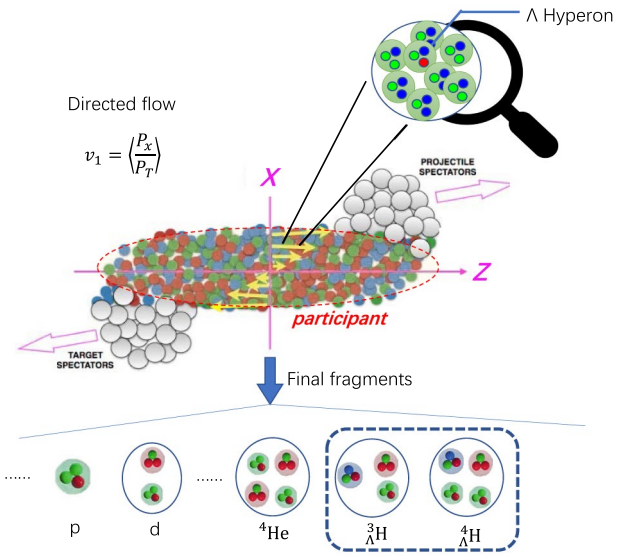

Fig. 1 (Color online) A carton for hypernuclei collective flow in high-energy heavy ion collisions

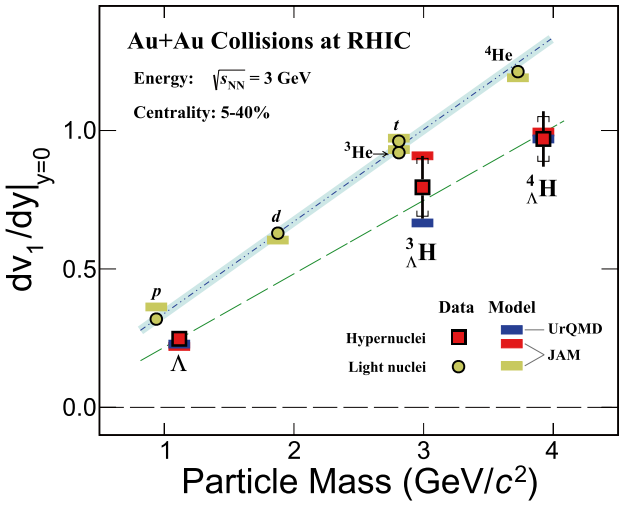

Fig. 2 (Color online) Mass dependence of the mid-rapidity v_1 slope, dv_1/dy, for Λ, $^3_\Lambda$H and $^4_\Lambda$H from the $\sqrt{s_{NN}}$ = 3 GeV 5–40% mid-central Au+Au collisions. Transport models (JAM model and UrQMD model) plus coalescence afterburner can describe the data. The figure is taken from Ref. [40]

minimum bias (MB) events are used for this analysis. $^3_\Lambda$H is reconstructed via both two-body and three-body decays $^3_\Lambda\mathrm{H} \to {}^3\mathrm{He} + \pi^-$ and $^3_\Lambda\mathrm{H} \to d + p + \pi^-$ while $^4_\Lambda$H is reconstructed via the two-body decay channel, $^4_\Lambda\mathrm{H} \to {}^4\mathrm{He} + \pi^-$. For this analysis, a relatively wide centrality range, 5–40%, is selected where both the event plane resolution and the yields of hypernuclei are maximized.

The Time-Projection Chamber (TPC) [36] is the main sub-detector for identifying above decay daughters, which is the main tracking detector in STAR, is 4.2 m long and 4 m in diameter, positioned inside a 0.5 T solenoidal magnetic field along the beam direction. Charged particles, including π^-, p, d, ^{3}He and ^{4}He, are selected based on the ionization energy loss (dE/dx) measured in the TPC as a function of rigidity (p/|q|), where p and q are the momentum and charge of the particle. In order to ensure high track quality, the number of TPC points used in the track fitting is required to be larger than 15 (out of a maximum of 45). Λ, $^3_\Lambda$H and $^4_\Lambda$H were reconstructed using the KFParticle package based on a Kalman filter method [37, 38].

Signal candidates of Λ, $^3_\Lambda$H and $^4_\Lambda$H were obtained via their invariant mass distributions reconstructed from decay daughters. The directed flow of Λ, $^3_\Lambda$H and $^4_\Lambda$H are extracted with the event plane method [39]. In transverse momentum (p_t) interval of $0.4 < p_t/A < 0.8$ GeV/c (hypernucleus is very close to this p_t interval due to the statistical reason), Λ, $^3_\Lambda$H and $^4_\Lambda$H v_1 as a function of rapidity (y) is obtained from 5 to 40% mid-central Au + Au collisions at $\sqrt{s_{NN}} = 3$ GeV. In the Ref. [35], the $v_1(y)$ of p, d, t, ^{3}He and ^{4}He from the same data are also analyzed in the p_t interval of $0.4 < p_t/A < 0.8$ GeV/c. Due to limited statistics, the $v_1(y)$ distributions of hypernuclei are fitted with a linear function $v_1(y) = a{\cdot}y$, in the rapidity range $-1.0 < y < 0.0$. $v_1(y)$ of Λ, p, d, t, ^{3}He and ^{4}He are fitted with a third-order polynomial function $v_1(y) = a{\cdot}y + b{\cdot}y^3$ in the rapidity regions, where a stands for the mid-rapidity slope $dv_1/dy|_{y=0}$, and b are fitting parameters.

The mid-rapidity slopes dv_1/dy for Λ, $^3_\Lambda$H and $^4_\Lambda$H as a function of particle mass are shown in Fig. 2. In same 5–40% data, v_1 slopes of p, d, t, ^{3}He and ^{4}He are presented by open circles. The slopes dv_1/dy of hypernuclei are all systematically lower than these of nuclei with the same mass number. Linear fits are performed on the mass dependence of dv_1/dy for both light nuclei and hypernuclei. The obtained slope parameters are 0.3323 ± 0.0003 for light nuclei and 0.27 ± 0.04 for hypernuclei, respectively. Two transport models (JAM and UrQMD) plus coalescence afterburner calculations are in agreement with data within uncertainties. These observations suggest that coalescence of nucleons and hyperon Λ could be the dominant mechanism for the hypernuclei $^3_\Lambda$H and $^4_\Lambda$H production in the 3 GeV collisions.

With the uncertainties, it seems that the mass dependence of the hypernuclei v_1 slope is similar to that of light nuclei although it may not necessarily be so due to the differences in N-N and Y–N interactions. In future, precision data on hypernuclei collectivity will yield invaluable insights on in-medium Y–N interaction. This work opens up a new direction for studying Y–N interaction under finite pressure [41]. This is important for making connection between heavy-ion collisions and the equation of state which governs the inner structure of compact stars. The excitation function of hypernuclei collective flow would provide valuable information

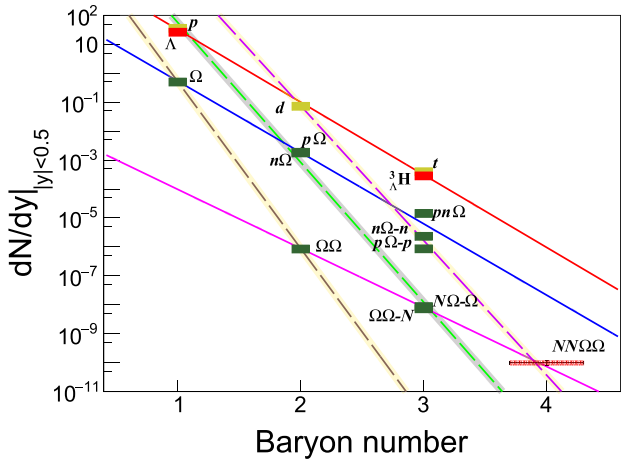

Fig. 3 (Color online) The exponential decay relation of dN/dy versus the constituent mass number (A) for Pb + Pb collisions at 2.76 TeV. There are basically two-class production chains, i.e. the one is: $N \to d \to t$ ($^3_\Lambda$H) (red), $\Omega \to N\Omega \to NN\Omega$ (blue), $\Omega\Omega \to N\Omega\Omega$ (pink), and the another is: $N \to N\Omega \to N\Omega\Omega$ (green), $\Omega \to \Omega\Omega$ (brown) and $d \to N\Omega N \to NN\Omega\Omega$ (violet). Lines show the exponential decay fits. The figure is adapted from Ref. [42]

for understanding in-medium Y–N interactions, which can be achieved in STAR BES-II program in future.

Last but not least, it is worthy to mention that the production of multi-strangeness hypernuclei is another important probe to understand Y–N as well as Y–Y interactions. In a recent work on multi-strangeness hypernuclei production by Zhang et al. [42], nucleon and Ω which has triple strange quarks, are coalesced into ΩNN and ΩΩN based on the phase-space information generated by the blast-wave model. It is found that with the growing of constituent baryon number, e.g. $\Omega \to N\Omega \to NN\Omega$ as well as $N \to N\Omega \to \Omega\Omega N$, the production rates appear to follow the exponential function $\exp(-cA)$ where c is the reduction factor. This kind of baryon number dependent trend is similar to that for light nuclei of $p \to d \to t$ ($^3_\Lambda$H) in Fig. 3. In general, two classes for these production chains are observed. One is for $N \to d \to t$ ($^3_\Lambda$H), $\Omega \to N\Omega \to NN\Omega$ and $\Omega\Omega \to N\Omega\Omega$ (solid lines). Another is for $N \to N\Omega \to N\Omega\Omega$, $\Omega \to \Omega\Omega$ and $d \to NN\Omega$ chains (dash lines). The fact that much larger reduction of dN/dy for the second class than the first class illustrates that much less yield for adding one more Ω than one more nucleon, which mainly results from the different interactions between N-Ω and Ω-Ω. Thus, the production of hypernuclei could provide another method to understand the hyperons and nucleons interactions. Interestingly, different magnitude and slopes for baryon number dependence of hypernuclei production [42] as well as mid-rapidity v_1 slope between light nuclei and hypernuclei [35] are exhibited, demonstrating rich information on N–N, Y–N and Y–Y–N interactions. Overall, systematic studies on hypernuclei will build a connection between nuclear collisions and the equation of state which governs the inner structure of compact stars.

References

1. H.T. Cromartie et al., Relativistic Shapiro delay measurements of an extremely massive millisecond pulsar. Nat. Astron. **4**, 72–76 (2019). https://doi.org/10.1038/s41550-019-0880-2
2. Y. Zhang, D. Zhang, X. Luo, Experimental study of the QCD phase diagram in relativistic heavy-ion collisions. Nucl. Tech. **46**, 040001 (2023). https://doi.org/10.11889/j.0253-3219.2023.hjs.46.040001. (**in Chinese**)
3. K. Sun, L. Chen, C.M. Ko et al., Light nuclei production and QCD phase transition in heavy-ion collisions. Nucl. Tech. **46**, 040012 (2023). https://doi.org/10.11889/j.0253-3219.2023.hjs.46.040012. (**in Chinese**)
4. B.I. Abelev et al., Observation of an antimatter hypernucleus. Science **328**, 58 (2010). https://doi.org/10.1126/science.1183980
5. H. Agakishiev et al., Observation of the antimatter helium-4 nucleus. Nature **473**, 353 (2011). https://doi.org/10.1038/nature10079
6. J. Adam et al., Measurement of the mass difference and the binding energy of the hypertriton and antihypertriton. Nat. Phys. **16**, 409 (2020). https://doi.org/10.1038/s41567-020-0799-7
7. J. Chen, D. Keane, Y.G. Ma et al., Antinuclei in heavy-ion collisions. Phys. Rep. **760**, 1 (2018). https://doi.org/10.1016/j.physrep.2018.07.002
8. M. Abdulhamid, B. Aboona, J. Adam et al., Beam energy dependence of triton production and yield ratio ($N_t \times N_p/N_d^2$) in Au + Au collisions at RHIC. Phys. Rev. Lett. **130**, 202301 (2023). https://doi.org/10.1103/PhysRevLett.130.202301
9. C.M. Ko, Searching for QCD critical point with light nuclei. Nucl. Sci. Tech. **34**, 80 (2023). https://doi.org/10.1007/s41365-023-01231-1
10. L. Adamczyk et al., Measurement of interaction between antiprotons. Nature **527**, 345 (2015). https://doi.org/10.1038/nature15724
11. S. Acharya et al., Unveiling the strong interaction among hadrons at the LHC. Nature **588**, 232 (2020). https://doi.org/10.1038/s41586-020-3001-6
12. M.S. Abdallah et al., Pattern of global spin alignment of ϕ *and* k^{*0} mesons in heavy-ion collisions. Nature **614**, 244 (2023). https://doi.org/10.1038/s41586-022-05557-5
13. X.N. Wang, Vector meson spin alignment by the strong force field. Nucl. Sci. Tech. **34**, 15 (2023). https://doi.org/10.1007/s41365-023-01166-7
14. J. Chen, Z.T. Liang, Y.G. Ma et al., Global spin alignment of vector mesons and strong force fields in heavy-ion collisions. Sci. Bull. **68**, 874 (2023). https://doi.org/10.1016/j.scib.2023.04.001
15. A. Andronic, P. Braun-Munzinger, J. Stachel et al., Production of light nuclei, hypernuclei and their antiparticles in relativistic nuclear collisions. Phys. Lett. B **697**, 203–207 (2011). https://doi.org/10.1016/j.physletb.2011.01.053
16. J. Steinheimer et al., Hypernuclei, dibaryon and antinuclei production in high energy heavy ion collisions: Thermal production vs. Coalescence. Phys. Lett. B **714**, 85–91 (2012). https://doi.org/10.1016/j.physletb.2012.06.069
17. J. Aichelin et al., Parton-hadron-quantum-molecular dynamics: a novel microscopic n -body transport approach for heavy-ion collisions, dynamical cluster formation, and hypernuclei production. Phys. Rev. C **101**, 044905 (2020). https://doi.org/10.1103/PhysRevC.101.044905

18. C.M. Hung, E.V. Shuryak, Hydrodynamics near the QCD phase transition: looking for the longest lived fireball. Phys. Rev. Lett. **75**, 4003–4006 (1995). https://doi.org/10.1103/PhysRevLett.75.4003
19. J. Brachmann et al., Antiflow of nucleons at the softest point of the EoS. Phys. Rev. C **61**, 024909 (2000). https://doi.org/10.1103/PhysRevC.61.024909
20. J. Steinheimer, J. Auvinen, H. Petersen et al., Examination of directed flow as a signal for a phase transition in relativistic nuclear collisions. Phys. Rev. C **89**, 054913 (2014). https://doi.org/10.1103/PhysRevC.89.054913
21. Y. Nara, H. Niemi, A. Ohnishi et al., Examination of directed flow as a signature of the softest point of the equation of state in QCD matter. Phys. Rev. C **94**, 034906 (2016). https://doi.org/10.1103/PhysRevC.94.034906
22. T.Z. Yan, Y.G. Ma, X.Z. Cai et al., Scaling of anisotropic flow and momentum-space densities for light particles in intermediate energy heavy ion collisions. Phys. Lett. B **638**, 50 (2006). https://doi.org/10.1016/j.physletb.2006.05.018
23. C.Z. Shi, Y.G. Ma, alpha-clustering effect on flows of direct photons in heavy-ion collisions. Nucl. Sci. Tech. **32**, 66 (2021). https://doi.org/10.1007/s41365-021-00897-9
24. J.H. Chen, Y.G. Ma, G.L. Ma et al., Elliptic flow of ϕ meson and strange quark collectivity. Phys. Rev. C **74**, 064902 (2006). https://doi.org/10.1103/PhysRevC.74.064902
25. H. Wang, J.H. Chen, Anisotropy flows in Pb-Pb collisions at lhc energies from parton scatterings with heavy quark trigger. Nucl. Sci. Tech. **33**, 15 (2022). https://doi.org/10.1007/s41365-022-00999-y
26. L.X. Han, G.L. Ma, Y.G. Ma et al., Initial fluctuation effect on harmonic flows in high-energy heavy-ion collisions. Phys. Rev. C **84**, 064907 (2011). https://doi.org/10.1103/PhysRevC.84.064907
27. S.W. Lan, S.S. Shu, Anisotropic flow in high baryon density region. Nucl. Sci. Tech. **33**, 21 (2022). https://doi.org/10.1007/s41365-022-01006-0
28. M. Wang, J.Q. Tao, H. Zheng et al., Number-of-constituent-quark scaling of elliptic flow: a quantitative study. Nucl. Sci. Tech. **33**, 37 (2022). https://doi.org/10.1007/s41365-022-01019-9
29. L. Adamczyk et al., Beam-energy dependence of the directed flow of protons, antiprotons, and pions in Au+Au collisions. Phys. Rev. Lett. **112**, 162301 (2014). https://doi.org/10.1103/PhysRevLett.112.162301
30. L. Adamczyk et al., Beam-energy dependence of directed flow of Λ, $\bar{\Lambda}$, $K^{\pm}$, K^0_s and ϕ in Au+Au collisions. Phys. Rev. Lett. **120**, 062301 (2018). https://doi.org/10.1103/PhysRevLett.120.062301
31. J. Adam et al., Beam-energy dependence of the directed flow of deuterons in Au+Au collisions. Phys. Rev. C **102**, 044906 (2020). https://doi.org/10.1103/PhysRevC.102.044906
32. L. Adamczyk et al., Elliptic flow of identified hadrons in Au+Au collisions at $\sqrt{s_{NN}}$ = 7.7–62.4 GeV. Phys. Rev. C **88**, 014902 (2013). https://doi.org/10.1103/PhysRevC.88.014902
33. J. Adam et al., Flow and interferometry results from Au+Au collisions at $\sqrt{s_{NN}}$ = 4.5 GeV. Phys. Rev. C **103**, 034908 (2021). https://doi.org/10.1103/PhysRevC.103.034908
34. A. Bzdak et al., Mapping the phases of quantum chromodynamics with beam energy scan. Phys. Rept. **853**, 1–87 (2020). https://doi.org/10.1016/j.physrep.2020.01.005
35. B.E. Aboona et al., Observation of Directed Flow of Hypernuclei ${}^3_\Lambda$H and ${}^3_\Lambda$H in $\sqrt{s_{NN}}$ = 3 GeV Au+Au Collisions at RHIC. Phys. Rev. Lett. **130**, 212301 (2023). https://doi.org/10.1103/PhysRevLett.130.212301
36. M. Anderson et al., The STAR time projection chamber: a Unique tool for studying high multiplicity events at RHIC. Nucl. Instrum. Meth. A **499**, 659–678 (2003). https://doi.org/10.1016/S0168-9002(02)01964-2
37. I. Kisel, Event Topology Reconstruction in the CBM Experiment. J. Phys. Conf. Ser. **1070**, 012015 (2018). https://doi.org/10.1088/1742-6596/1070/1/012015
38. M. Zyzak, Online selection of short-lived particles on many-core computer architectures in the CBM experiment at FAIR. Ph.D. thesis, Frankfurt U. (2016)
39. H. Masui, A. Schmah, A.M. Poskanzer, Event plane resolution correction for azimuthal anisotropy in wide centrality bins. Nucl. Instrum. Meth. A **833**, 181–185 (2016). https://doi.org/10.1016/j.nima.2016.07.037
40. B.E. Aboona et al., Observation of directed flow of hypernuclei ${}^3_\Lambda$H and ${}^4_\Lambda$H in $\sqrt{s\mathrm{NN}}$ = 3 GeV Au + Au Collisions at RHIC. Phys. Rev. Lett. **130**, 212301 (2023). https://doi.org/10.1103/PhysRevLett.130.212301
41. T. Neidig, K. Gallmeister, C. Greiner et al., Towards solving the puzzle of high temperature light (anti)-nuclei production in ultra-relativistic heavy ion collisions. Phys. Lett. B **827**, 136891 (2022). https://doi.org/10.1016/j.physletb.2022.136891
42. L. Zhang, S. Zhang, Y.G. Ma, Production of ΩNN and $\Omega\Omega N$ in ultra-relativistic heavy-ion collisions. Eur. Phys. J. C **82**, 416 (2022). https://doi.org/10.1140/epjc/s10052-022-10336-7